^{35}Cl NQR, Crystal Structure, and Pyroelectricity of 2,3-Dichloro-1,4-naphthoquinone *

Stefanie Brummer**, Ulrich Sohling, and Alarich Weiss

Institut für Physikalische Chemie, Physikalische Chemie III, Technische Hochschule Darmstadt, Darmstadt, West Germany

Z. Naturforsch. **45a,** 259–267 (1990); received August 7, 1989

The ^{35}Cl NQR spectra of the two phases (phases I and II) of 2,3-dichloro-1,4-naphthoquinone were studied from 77 to 394 K. The crystal structure determination of the triclinic phase (phase I) was refined by single crystal X-ray diffraction. Phase I crystallizes in the space group C_i^1-$P\bar{1}$. The unit cell ($Z=4$) has the dimensions $a=1614.3(4)$ pm, $b=828.1(3)$ pm, $c=733.2(3)$ pm, $\alpha=67.02(1)°$, $\beta=82.55(1)°$, $\gamma=89.77(1)°$. In the temperature range $439 \leqq T_{\mathrm{I}\to\mathrm{II}}/\mathrm{K} \leqq 447$ a unidirectional phase transition I → II is observed. Phase II is orthorhombic, space group C_{2v}^5-$Pb2_1a$. The bond distances $d_{(\mathrm{C-Cl})}$ and the ^{35}Cl NQR frequencies correlate quite well according to the theory: $\nu(^{35}\mathrm{Cl}) \sim (d_{(\mathrm{C-Cl})})^{-3}$. The multiplicity of the ^{35}Cl NQR spectra is discussed.

Pyroelectricity studies on phase II are reported. The pyroelectric coefficient depends little on the temperature, $8.3 \leqq p^x/\mu\mathrm{C\,m^{-2}\,K^{-1}} \leqq 10.7$ in $103 \leqq T/\mathrm{K} \leqq 343$.

Introduction

The existence of two solid phases of 2,3-dichloro-1,4-naphthoquinone (2,3-Cl_2-1,4-$O_2C_{10}H_4$) is reported in [1, 2]. Phase I grows from toluene solution and crystallizes triclinic (space group C_i^1-$P\bar{1}$). The crystal structure of I was determined by Métras [1]. The second modification of $C_{10}H_4Cl_2O_2$, phase II, is orthorhombic (space group C_{2v}^5-$Pb2_1a$), $Z=8$. It is obtained by growing the crystals from the melt. Ikemoto et al. [2] determined the crystal structure of II. The main structural difference between the two solid phases is the relative orientations of the neighbouring molecules to each other. A molecule of 2,3-Cl_2-1,4-$O_2C_{10}H_4$ has a permanent dipole moment $\boldsymbol{\mu}$ directed along its twofold molecular axis. In the triclinic phase I two neighbouring molecules are connected by a common centre of symmetry whereby the molecular dipole moments are cancelled. In the orthorhombic phase II all molecular dipole moments are directed nearly parallel, creating a net dipole moment of a crystal of 2,3-Cl_2-1,4-$O_2C_{10}H_4$.

In this paper we report on ^{35}Cl NQR experiments on polycrystalline 2,3-Cl_2-1,4-$O_2C_{10}H_4$ (I and II) and on the pyroelectricity of II. The crystal structure determination [1] of I has been refined at 298 K.

Experimental

Preparation

2,3-Dichloro-1,4-naphthoquinone, 2,3-Cl_2-1,4-$O_2C_{10}H_4$ (Aldrich Chemistry, 98%) was purified by sublimation in vacuo, and thereafter by recrystallization, once from ethanol and three times from toluene. Phase I was obtained by crystallization from toluene and II was grown from the melt by Bridgeman technique.

For the determination of the pyroelectric coefficient, crystals of II were cut in thin slices with the normal of the plates parallel to the polar axis (***b***-axis).

^{35}Cl NQR

The ^{35}Cl NQR spectra of the two phases were registered as functions of temperature by use of a pulsed NQR Fourier Transform (FT) spectrometer. The measurements of $\nu(^{35}\mathrm{Cl})=f(T)$ were done by heating or cooling the sample to the desired temperature with a stream of temperature regulated N_2 gas or air. The temperature at the sample was measured with

---

* Presented at the Xth International Symposium on Nuclear Quadrupole Resonance Spectroscopy, Takayama, Japan, August 22–26, 1989.

** Part of Dr.-Ing. Dissertation of Stefanie Brummer, Technische Hochschule Darmstadt (D 17).

Reprint requests to Prof. Dr. Al. Weiss, Institut für Physikalische Chemie III, Technische Hochschule Darmstadt, Petersenstraße 20, D-6100 Darmstadt.

0932-0784 / 90 / 0300-0259 $ 01.30/0. – Please order a reprint rather than making your own copy.

Table 1. Experimental conditions for the crystal structure determination and crystallographic data of 2,3-dichloro-1,4-naphthoquinone (phase I).

Formula		$C_{10}H_4O_2Cl_2$
Molecular mass, g/mol		227.05
Crystal habitus		prism
Size/mm^3		$0.22 \times 0.38 \times 1.0$
Colour		yellow
Diffractometer		Stoe-Stadi-4
Wavelength, λ/pm		71.069 (Mo Kα)
$(\sin \vartheta/\lambda)_{max}$/pm^{-1}		0.005947
Monochromator		graphite (002)
Temperature, T/K		298
Linear absorption coefficient, μ/m^{-1}		618
Lattice constants	a/pm	1614.3(4)
	b/pm	828.1(3)
	c/pm	733.2(3)
	α/°	67.02(1)
	β/°	82.55(1)
	γ/°	89.77(1)
Volume of the unit cell	$V \cdot 10^{-6}$/pm^3	893.57
Space group	C_i^1-$P\bar{1}$	
Formula units/unit cell		$Z=4$
$\varrho_{calc}/(\mathrm{Mg \cdot m^{-3}})$		1.688
$\varrho_{pykn}/(\mathrm{Mg \cdot m^{-3}})$		1.68
Scan	$\omega/2\theta$	numbering of atoms in the molecule
Number of measured reflections	3548	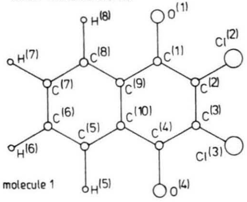
Symmetry independent reflections	3128	
Reflections considered	2879	
Number of free parameters	278	
$F(000)$	456	
$R(F)$	0.0341	
$R_w(F)$	0.0315	The numbering of molecule **2** is identical exept the numbers are pointed.
Point positions, all atoms in $2i$:	$x, y, z;$ $\bar{x}, \bar{y}, \bar{z}.$	Molecule **1**→molecule **2**: $C^{(n)} \rightarrow C^{(n')}$, $H^{(n)} \rightarrow H^{(n')}$, $Cl^{(n)} \rightarrow Cl^{(n')}$, and $O^{(n)} \rightarrow O^{(n')}$.

a copper-constantan thermocouple to ±0.3 K. The frequencies measured are accurate to ±0.003 MHz.

Differential Thermal Analysis

Differential scanning calorimetry (DSC) and differential thermal analysis (DTA) (20 °C → 240 °C → 20 ° → 240 °C) were carried out for both phases. The melting point T_M of 2,3-Cl_2-1,4-$O_2C_{10}H_4$ is 193 ± 0.5 °C. By DTA $T_M = 193.6$ °C was found for II and $T_M = 192.5$ °C by heating I. From DSC we found an enthalpy of melting, $\Delta\bar{H}_M \approx 25$ kJ mol^{-1} (24.6 kJ mol^{-1} for II, 25.0 kJ mol^{-1} for I as the start material). In the DTA curve (first cycle 20 °C → 240 °C) of I a weak peak was observed at 166 °C with the enthalpy change $\Delta\bar{H} \approx 0.17$ kJ mol^{-1}. ^{35}Cl NQR measurements on annealed samples of I (8 h at T/°C = 149, 163, 169, 174, 180) have shown that a solid → solid phase transition occurs in 2,3-Cl_2-1,4-$O_2C_{10}H_4$. By means of ^{35}Cl NQR spectra of the annealed samples, measured at room temperature, we observed the transition I → II at $166 \leqq T/°C \leqq 174$. From these experiments we conclude: Phase I of 2,3-Cl_2-1,4-$O_2C_{10}H_4$ is a metastable phase which transforms to II at $166 \leqq T_{I \rightarrow II}/°C \leqq 174$ with a small transition enthalpy. The melting point of II is (193 ± 1) °C. Phase II is the thermodynamically stable phase of the compound.

Crystal Structure Analysis

The crystal structure of I was determined by the single crystal technique at room temperature using Mo Kα-radiation. The experimental details and the crystallographic data are given in Table 1.

Pyroelectricity

For the determination of the pyroelectric coefficient, at constant stress x, p^x of crystalline solids, single crystals were cut in thin slices with the normal of the plate parallel to the polar axis. Then

$$p^x = \frac{\mathrm{d}Q/\mathrm{d}t}{A(\mathrm{d}T/\mathrm{d}t)} = \frac{I}{A(\mathrm{d}T/\mathrm{d}t)} = \frac{U}{AR(\mathrm{d}T/\mathrm{d}t)}, \quad (1)$$

where A is the area of the crystal plate, T its temperature, t the time, Q the electric charge, I the current, U the voltage, and R the electric resistance. For a given p^x, the voltage measured on the resistance R is proportional to the area of the crystal plate and to the variation of T with time. The crystal plate was contacted, with an air drying silver paste, and connected to the measuring circuit. The following, most common two methods of creating $\mathrm{d}T/\mathrm{d}t$ and measuring U were used [3]: (a) p^x is measured at constant rate of temperature change, $\mathrm{d}T/\mathrm{d}t = \mathrm{const}$. From the measured I (respectively U, R, A, and $\mathrm{d}T/\mathrm{d}t$) p^x is calculated [4]. (b) $\mathrm{d}T/\mathrm{d}t$ is a periodic function. The pyroelectric voltage is measured as $U = U_0 \cos \omega t$. A periodic $\mathrm{d}T/\mathrm{d}t$ was generated via a Peltier element [5].

Results

Crystal Structure of Phase I

In Table 1 the crystallographic data of I are given together with some experimental details. Table 2 lists

Table 2. Positional and thermal parameters (with standard deviations) of 2,3-dichloro-1,4-naphthoquinone, phase I. The temperature factors are of the form:

$T = \exp[-2\pi^2(U_{11} \cdot h^2 \cdot a^{*2} + U_{22} \cdot k^2 \cdot b^{*2} + U_{33} \cdot l^2 \cdot c^{*2} + 2U_{12} \cdot h \cdot k \cdot a^* \cdot b^* + 2U_{13} \cdot h \cdot l \cdot a^* \cdot c^* + 2U_{23} \cdot k \cdot l \cdot b^* \cdot c^*)]$.

U and U_{ij} are given in pm^2.

Atom	x/a	y/b	z/c	U_{11} or U	U_{22}	U_{33}	U_{23}	U_{13}	U_{12}
Molecule **1**									
Cl$^{(2)}$	0.2331(0)	0.8369(1)	0.2144(1)	343(3)	648(4)	1005(6)	−389(4)	−129(3)	53(3)
Cl$^{(3)}$	0.1197(0)	0.5182(1)	0.2358(1)	593(4)	372(3)	763(5)	−263(3)	−42(3)	106(3)
C$^{(1)}$	0.0913(1)	1.0089(3)	0.2319(3)	425(12)	348(11)	409(13)	−163(10)	−91(10)	−4(9)
C$^{(2)}$	0.1268(1)	0.8418(3)	0.2331(3)	335(11)	383(12)	454(12)	−168(10)	−65(10)	25(9)
C$^{(3)}$	0.0789(1)	0.7062(2)	0.2444(3)	423(12)	306(11)	428(13)	−167(10)	−40(10)	42(9)
C$^{(4)}$	−0.0146(1)	0.7102(3)	0.2617(3)	428(12)	359(11)	390(13)	−176(10)	−11(10)	−39(9)
C$^{(5)}$	−0.1385(1)	0.8837(3)	0.2863(4)	379(13)	534(14)	519(15)	−242(12)	−34(11)	13(10)
H$^{(5)}$	−0.1731(12)	0.7752(25)	0.3011(31)	500(0)					
C$^{(6)}$	−0.1737(1)	1.0340(3)	0.2892(4)	385(13)	664(16)	537(16)	−230(13)	−59(12)	124(12)
H$^{(6)}$	−0.2327(12)	1.0412(25)	0.3047(32)	500(0)					
C$^{(7)}$	−0.1239(2)	1.1761(3)	0.2727(4)	593(16)	486(14)	524(16)	−232(13)	−96(13)	211(12)
H$^{(7)}$	−0.1468(12)	1.2885(25)	0.2687(31)	500(0)					
C$^{(8)}$	−0.0378(1)	1.1685(3)	0.2520(3)	546(15)	348(12)	453(14)	−184(11)	−90(12)	47(10)
H$^{(8)}$	0.0012(12)	1.2652(25)	0.2356(30)	450(0)					
C$^{(9)}$	−0.0014(1)	1.0159(2)	0.2501(3)	395(11)	323(10)	338(12)	−140(9)	−72(10)	28(9)
C$^{(10)}$	−0.0518(1)	0.8731(2)	0.2670(3)	382(12)	364(11)	334(12)	−150(9)	−34(9)	6(9)
O$^{(1)}$	0.1366(1)	1.1310(2)	0.2155(3)	488(10)	413(9)	880(14)	−304(9)	−126(9)	−92(7)
O$^{(4)}$	−0.0564(1)	0.5861(2)	0.2704(3)	515(10)	438(9)	865(14)	−359(9)	13(9)	−122(8)
Molecule **2**									
Cl$^{(2')}$	0.6150(0)	0.8507(1)	0.1970(1)	571(4)	386(3)	675(4)	−273(3)	−42(3)	58(3)
Cl$^{(3')}$	0.7309(0)	0.5393(1)	0.2130(1)	350(3)	677(4)	1081(6)	−461(4)	−132(4)	56(3)
C$^{(1')}$	0.4826(1)	0.6302(3)	0.2460(3)	412(12)	340(11)	402(13)	−166(10)	−51(10)	64(9)
C$^{(2')}$	0.5754(1)	0.6500(2)	0.2245(3)	428(12)	334(11)	377(12)	−171(10)	−44(10)	1(9)
C$^{(3')}$	0.6247(1)	0.5182(3)	0.2310(3)	352(12)	387(12)	456(13)	−200(10)	−63(10)	39(9)
C$^{(4')}$	0.5901(1)	0.3436(3)	0.2520(3)	426(13)	352(11)	480(14)	−203(10)	−73(11)	92(10)
C$^{(5')}$	0.4631(1)	0.1640(3)	0.2833(3)	522(14)	353(12)	479(14)	−199(11)	−72(12)	52(10)
H$^{(5')}$	0.4992(12)	0.0675(24)	0.2900(30)	450(0)					
C$^{(6')}$	0.3777(2)	0.1410(3)	0.2970(4)	574(16)	429(13)	515(15)	−200(12)	−77(12)	92(11)
H$^{(6')}$	0.3539(12)	0.0336(26)	0.3081(32)	500(0)					
C$^{(7')}$	0.3265(1)	0.2772(3)	0.2906(4)	394(13)	566(15)	540(16)	−195(13)	−59(12)	58(11)
H$^{(7')}$	0.2654(12)	0.2611(25)	0.3000(32)	500(0)					
C$^{(8')}$	0.3608(1)	0.4352(3)	0.2745(4)	390(12)	439(13)	492(14)	−179(11)	−53(11)	59(10)
H$^{(8')}$	0.3248(12)	0.5343(25)	0.2687(31)	450(0)					
C$^{(9')}$	0.4468(1)	0.4597(2)	0.2616(3)	370(11)	330(11)	345(12)	−144(9)	−39(9)	40(9)
C$^{(10')}$	0.4984(1)	0.3223(2)	0.2662(3)	402(12)	308(11)	352(12)	−144(9)	−54(10)	41(9)
O$^{(1')}$	0.4394(1)	0.7479(2)	0.2537(3)	489(10)	421(9)	941(14)	−375(9)	−68(9)	144(7)
O$^{(4')}$	0.6363(1)	0.2277(2)	0.2550(3)	477(10)	462(9)	1043(16)	−381(10)	−110(10)	167(8)

the positional and thermal parameters of the atoms in the unit cell.

^{35}*Cl NQR*

The temperature dependence of the ^{35}Cl NQR frequencies of I is plotted in Figure 1. Phase I shows a four line spectrum with equal intensity for each line throughout the range $77 \leqq T/\mathrm{K} \leqq 394$. The frequency difference between ν_3 and ν_4 is small; at 77 K it is 17 kHz, but the difference decreases with increasing temperature to a hardly resolvable doublet with $\Delta\nu = 3$ kHz.

Phase II gives a four line ^{35}Cl NQR spectrum too, which is plotted as a function of temperature ($77 \leqq T/\mathrm{K} \leqq 394$) in Figure 2. There are no discontinuities in the $\nu(^{35}\mathrm{Cl}) = f(T)$ curves for both phases. The temperature dependence of the ^{35}Cl NQR frequencies was parameterized according to

$$\nu(^{35}\mathrm{Cl}) = \sum_{i=-1}^{2} a_i T^i, \qquad (2)$$

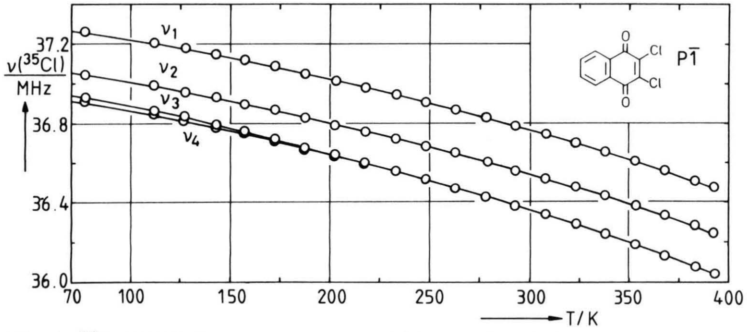

Fig. 1. ^{35}Cl NQR frequencies of 2,3-dichloro-1,4-naphthoquinone (phase I) as a function of temperature.

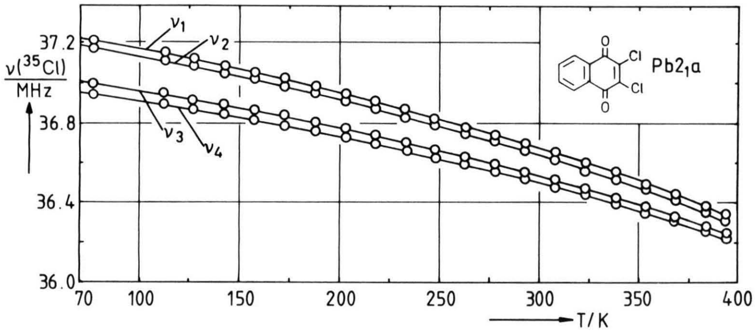

Fig 2. ^{35}Cl NQR frequencies of 2,3-dichloro-1,4-naphthoquinone (phase II) as a function of temperature.

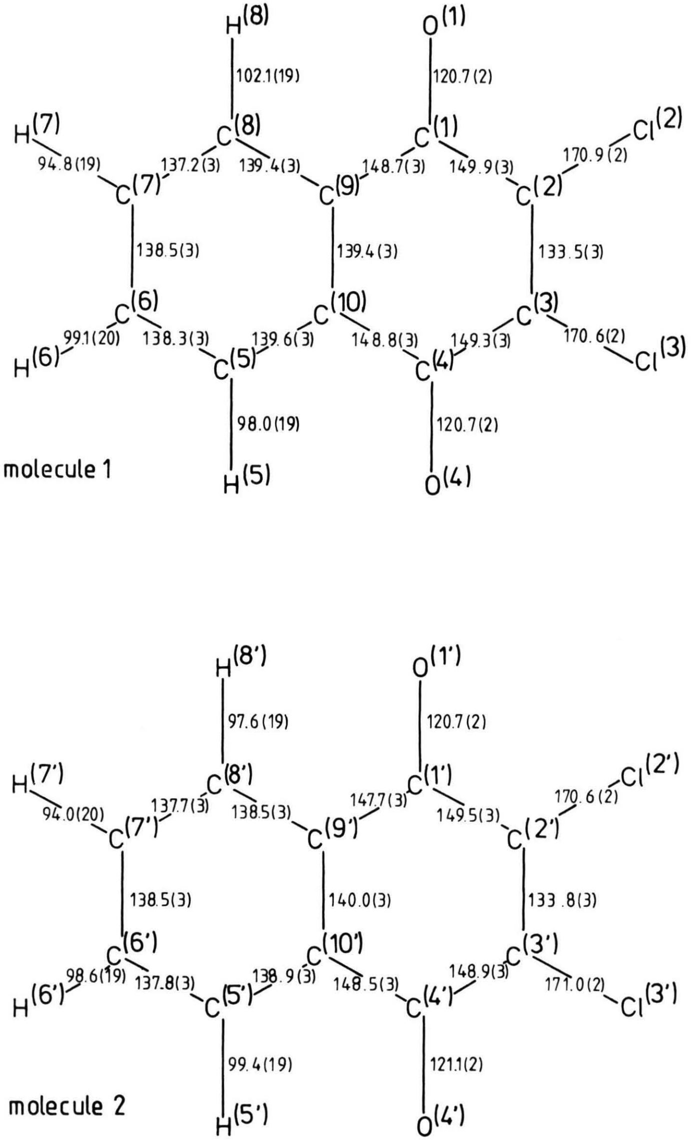

Fig. 5. Bond distances (in pm) the molecules of 2,3-dichloro-1,4-naphthoquinone of phase I (molecules **1** and **2**).

Table 3. Parametrization of $\nu(^{35}\text{Cl}) = f(T) = \sum a_i \cdot T^i$ $(-1 \leqq i \leqq 2)$ for phase I and phase II of 2,3-dichloro-1,4-naphthoquinone. Z = number of measurements, σ = standard deviation, $\Delta T = T_2 \ldots T_1$ is the temperature range of measurements.

^{35}Cl NQR line	Z	$\frac{\sigma}{\text{kHz}}$	$\frac{a_{-1}}{\text{MHz K}}$	$\frac{a_0}{\text{MHz}}$	$\frac{a_1 \cdot 10^6}{\text{MHz K}^{-1}}$	$\frac{a_2 \cdot 10^6}{\text{MHz K}^{-2}}$	$\frac{\Delta T}{\text{K}}$
Phase I							
ν_1	21	2.1	0.2611	37.3606	−1.1026	−2.9232	77 ... 393
ν_2	21	2.8	0.2690	37.1482	−1.1486	−2.9167	77 ... 393
ν_3	21	2.2	0.1048	37.0656	−1.5597	−2.6352	77 ... 394
ν_4	21	2.1	0.0964	37.0443	−1.4796	−2.6735	77 ... 394
Phase II							
ν_1	21	2.4	0.3457	37.3158	−1.1455	−3.3688	77 ... 394
ν_2	21	2.4	0.6499	37.2732	−1.1083	−3.4069	77 ... 394
ν_3	21	1.6	0.3371	37.1012	−1.0308	−2.9003	77 ... 394
ν_4	21	1.8	−1.2156	37.0549	−1.0049	−2.8305	77 ... 394

Table 4. ^{35}Cl NQR frequencies of 2,3-dichloro-1,4-naphthoquinone (phases I and II) at 77 K and at room temperature. The frequencies are given to ±0.003 MHz. The signal to noise ratio (S/N) is included. (The S/N ratio at 77 K is not 1:1:1:1, most probably caused by different relaxation times of the different chlorine atoms.)

Phase	^{35}Cl NQR line	$\frac{T}{\text{K}}$	$\frac{\nu(^{35}\text{Cl})}{\text{MHz}}$	$\frac{S}{N}$	$\frac{T}{\text{K}}$	$\frac{\nu(^{35}\text{Cl})}{\text{MHz}}$	$\frac{S}{N}$
I	ν_1	77	37.260	17	293.2	36.789	17
I	ν_2	77	37.044	13	293.2	36.562	17
I	ν_3	77	36.929	7	293.2	36.384	16
I	ν_4	77	36.912	13	293.2	36.381	17
II	ν_1	77	37.211	17	293.2	36.694	13
II	ν_2	77	37.175	8	293.2	36.660	10
II	ν_3	77	36.999	17	293.2	36.550	13
II	ν_4	77	36.947	10	293.2	36.514	13

the coefficients a_i being listed in Table 3. Table 4 gives frequencies at selected temperatures for both phases. An assignment $\nu(^{35}\text{Cl}) \leftrightarrow$ atomic position is not possible, even not qualitatively. One recognizes that in both phases there are two groups of frequencies (ν_1, ν_2, and ν_3, ν_4), but there is no possibility (NQR on polycrystalline material) to relate these frequencies to certain chlorine atoms $\text{Cl}^{(2)}$, $\text{Cl}^{(2')}$ and $\text{Cl}^{(3)}$, $\text{Cl}^{(3')}$ of the molecular structure.

Pyroelectric Coefficient of Phase II

The pyroelectric coefficient p^x was studied on six different crystal plates (area of the crystal plates: $A = (18-46)\ \text{mm}^2$, and thickness of the crystal plates: $d = (0.7-1.0)$ mm) in $100 \leqq T/\text{K} \leqq 344$. In Fig. 3 the pyroelectric coefficient p^x is plotted vs. temperature; we found $p^x = 8.3\ \mu\text{C m}^{-2}\ \text{K}^{-1}$ at 103 K and 10.7 $\mu\text{C m}^{-2}\ \text{K}^{-1}$ at 343 K.

Discussion

Crystal Structure and ^{35}Cl NQR

In the following, we first discuss the ^{35}Cl NQR spectra and the crystal structure of 2,3-Cl_2-1,4-$\text{O}_2\text{C}_{10}\text{H}_4$ in I.

Bray et al. [6] reported a single NQR line (ν(77 K) = 37.114 MHz) for I. In contrast, we observed a four line ^{35}Cl NQR spectrum, with equal intensities, in the whole temperature range studied ($77 \leqq T/\text{K} \leqq 394$). The smooth curves $\nu_i = f(T)$ ($i = 1, 2, 3, 4$) are characteristic for a solid without a phase transition over the temperature range covered.

The crystal stucture of I is reported in [1]. Métras described the structure of I within the centrosymmetric space group C_i^1-$P\bar{1}$ with $Z = 4$. His least squares refinement led to a reliability factor $R = 0.114$. The unit cell contains two molecules in the asymmetric unit and therefore four crystallographically dif-

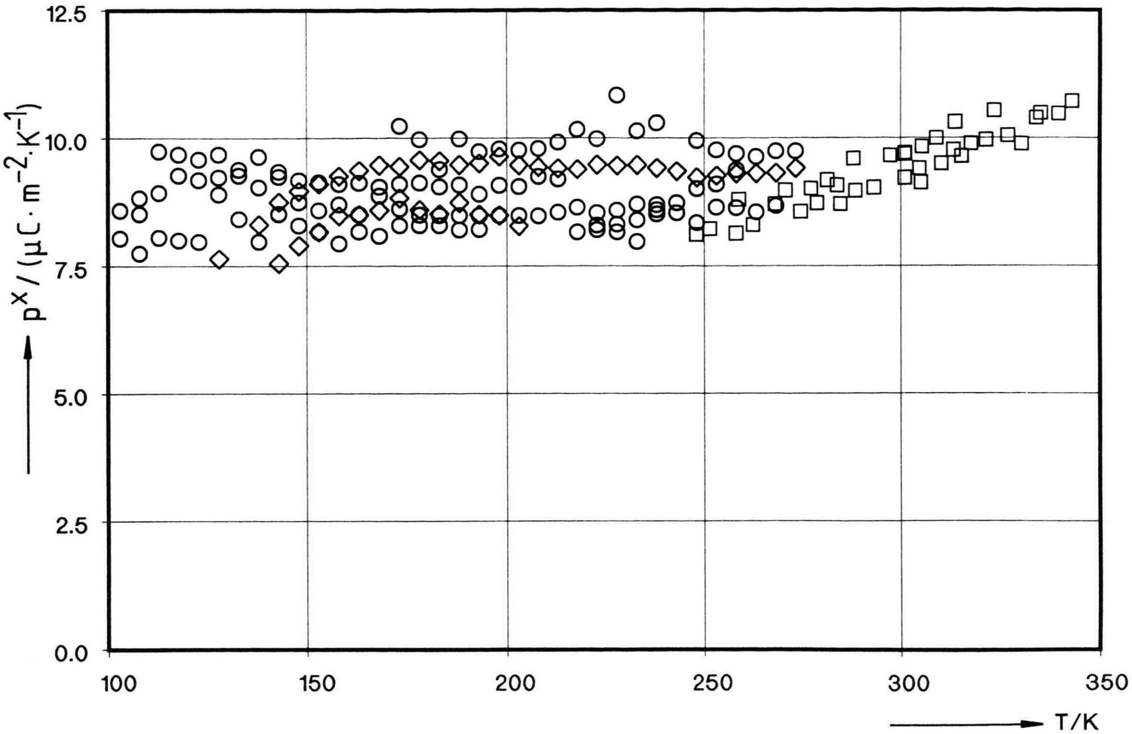

Fig. 3. Pyroelectric coefficient at constant stress, p^x, of 2,3-dichloro-1,4-naphthoquinone (phase II) as a function of temperature (○, ◇ measured with dT/dt = const. (◇ increasing temperature and ○ decreasing temperature), □ measured with dT/dt = periodic function).

ferent chlorine atoms; this fact is supported by the ^{35}Cl NQR spectrum. The bond lengths C–Cl within one molecule of I reported by [1] scatter strongly: $C^{(2)}-Cl^{(2)}$ = 176 pm and $C^{(3)}-Cl^{(3)} = 170$ pm, respectively $C^{(2')}-Cl^{(2')} = 178$ pm and $C^{(3')}-Cl^{(3')} = 171$ pm. Such large differences are very unlikely. For comparison: The C–Cl bond lengths in the tetrachloro-1,4-benzoquinone (chloranil) are 170.0 and 170.2 pm [7]. In II of 2,3-Cl_2-1,4-$O_2C_{10}H_4$ they are $C^{(2)}-Cl^{(2)} =$ 169.9 pm and $C^{(3)}-Cl^{(3)} = 172.7$ pm, respectively $C^{(2')}-Cl^{(2')}$ = 169.5 pm and $C^{(3')}-Cl^{(3')}$ = 170.1 pm [2]. The correlation of the NQR frequencies with the C–Cl bond lengths for chlorine bound to an sp^2 C-atom [8] shows that the C–Cl bond lengths are in the range $169 \leqq d/\text{pm} \leqq 174$.

We repeated the crystal structure determination of Métras [1]; the centrosymmetric space group C_i^1-$P\bar{1}$ was observed, too, with $r = 3.41\%$. The size of the unit cell measured is in agreement with the reported lattice constants [1] (our value; [1]: $V = 893.57 \cdot 10^6$ pm^3; $V = 901.96 \cdot 10^6$ pm^3). We note that the unit cell volume of II is $1780.29 \cdot 10^6$ pm^3. There is only a slight difference between the two phases ($V/Z = 223.39 \cdot 10^6$ pm^3 for I, $222.54 \cdot 10^6$ pm^3 for II).

In Fig. 4 the arrangement of the four molecules within the unit cell is shown in projection along the *c*-axis onto the plane (***ab***). There are two molecules in the asymmetric unit (molecules **1** and **2**). The molecules at site **1** are stacked along the *c*-axis ($c = 733.2$ pm) to form one molecular column, and those at site **2** form a second column, also along *c*. The column formed by the molecules **1** has its axis along ($x = 0$, $y = 0$, z), the column built by the molecules **2** along ($x = 1/2$, $y = 1/2$, z). The arrangement of the molecules in each column is significantly different from that in the orthorhombic form (II) [2].

All the molecules can be considered to be approximately planar. The best planes through the carbon atom skeleton of the naphthalene system are listed in Table 5, including the deviations of the atoms from these planes. The angle between the two planes (**1** and **2**) is 2.98°. The deviation of the atoms $Cl^{(2)}$, $Cl^{(3)}$, $O^{(1)}$

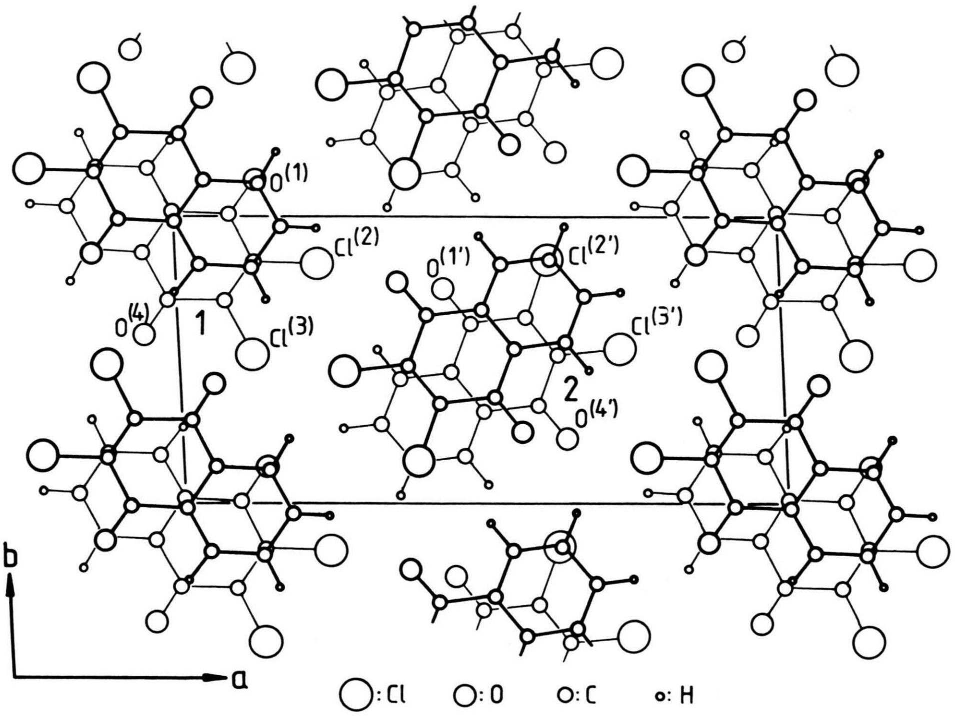

Fig. 4. Projection of the crystal structure of phase I of 2,3-dichloro-1,4-naphthoquinone along the ***c***-axis onto the plane (***a b***). A few atoms of the molecules (**1** and **2**) for which the coordinates are given in Table 2 are named (the molecules are marked by **1** and **2**).

Table 5. Best planes through the carbon atoms of the naphthalene ring in phase I of 2,3-dichloro-1,4-naphthoquinone. Deviations, *d*, of the atoms from these planes are given.

Atom	d/pm	Atom	d/pm
Molecule **1**		Molecule **2**	
$-0.0494\,x-0.3645\,y$ $+0.9299\,z=1.9432$		$-0.0808\,x-0.3250\,y$ $+0.9423\,z=2.4881$	
$\mathrm{Cl}^{(2)}$	4.82	$\mathrm{Cl}^{(2')}$	−6.13
$\mathrm{Cl}^{(3)}$	−4.38	$\mathrm{Cl}^{(3')}$	−1.82
$\mathrm{O}^{(1)}$	−1.79	$\mathrm{O}^{(1')}$	10.55
$\mathrm{O}^{(4)}$	−4.85	$\mathrm{O}^{(4')}$	0.58
$\mathrm{C}^{(1)}$	−0.02	$\mathrm{C}^{(1')}$	2.64
$\mathrm{C}^{(2)}$	2.15	$\mathrm{C}^{(2')}$	−2.27
$\mathrm{C}^{(3)}$	−0.13	$\mathrm{C}^{(3')}$	−0.65
$\mathrm{C}^{(4)}$	−1.90	$\mathrm{C}^{(4')}$	0.71
$\mathrm{C}^{(5)}$	0.80	$\mathrm{C}^{(5')}$	0.07
$\mathrm{C}^{(6)}$	1.11	$\mathrm{C}^{(6')}$	0.19
$\mathrm{C}^{(7)}$	0.32	$\mathrm{C}^{(7')}$	−1.38
$\mathrm{C}^{(8)}$	−1.43	$\mathrm{C}^{(8')}$	−0.29
$\mathrm{C}^{(9)}$	−0.92	$\mathrm{C}^{(9')}$	0.37
$\mathrm{C}^{(10)}$	0.02	$\mathrm{C}^{(10')}$	0.60

Table 6. Intermolecular contacts d/pm < 450 in phase I of 2,3-dichloro-1,4-naphthoquinone.

$\mathrm{Cl}^{(2)}\cdots\mathrm{O}^{(1')}$	343.2	$\mathrm{Cl}^{(3)}\cdots\mathrm{O}^{(1)}$	327.6	$\mathrm{Cl}^{(2')}\cdots\mathrm{O}^{(4')}$	333.6
$\mathrm{Cl}^{(2)}\cdots\mathrm{C}^{(6')}$	371.0	$\mathrm{Cl}^{(3)}\cdots\mathrm{O}^{(4)}$	339.2	$\mathrm{Cl}^{(2')}\cdots\mathrm{C}^{(6')}$	358.3
$\mathrm{Cl}^{(2)}\cdots\mathrm{Cl}^{(2')}$	372.1	$\mathrm{Cl}^{(3)}\cdots\mathrm{C}^{(8)}$	381.7	$\mathrm{Cl}^{(2')}\cdots\mathrm{C}^{(5')}$	373.8
$\mathrm{Cl}^{(2)}\cdots\mathrm{C}^{(8')}$	381.4	$\mathrm{Cl}^{(3)}\cdots\mathrm{C}^{(5)}$	382.2	$\mathrm{Cl}^{(2')}\cdots\mathrm{C}^{(5')}$	393.6
$\mathrm{Cl}^{(2)}\cdots\mathrm{O}^{(4')}$	401.6	$\mathrm{Cl}^{(3)}\cdots\mathrm{C}^{(10)}$	384.2	$\mathrm{Cl}^{(2')}\cdots\mathrm{C}^{(6)}$	398.0
$\mathrm{Cl}^{(2)}\cdots\mathrm{C}^{(6)}$	417.5	$\mathrm{Cl}^{(3)}\cdots\mathrm{C}^{(7')}$	386.8	$\mathrm{Cl}^{(2')}\cdots\mathrm{C}^{(7')}$	410.7
$\mathrm{Cl}^{(2)}\cdots\mathrm{C}^{(7')}$	421.1	$\mathrm{Cl}^{(3)}\cdots\mathrm{C}^{(8)}$	390.2	$\mathrm{Cl}^{(2')}\cdots\mathrm{C}^{(5)}$	414.2
$\mathrm{Cl}^{(2)}\cdots\mathrm{C}^{(7)}$	422.1	$\mathrm{Cl}^{(3)}\cdots\mathrm{C}^{(8')}$	397.7	$\mathrm{Cl}^{(2')}\cdots\mathrm{C}^{(4')}$	426.8
$\mathrm{Cl}^{(2)}\cdots\mathrm{C}^{(1')}$	436.8	$\mathrm{Cl}^{(3)}\cdots\mathrm{Cl}^{(3')}$	400.4	$\mathrm{O}^{(1')}\cdots\mathrm{C}^{(4')}$	336.9
$\mathrm{Cl}^{(3')}\cdots\mathrm{O}^{(4)}$	355.5	$\mathrm{O}^{(1)}\cdots\mathrm{C}^{(6)}$	347.8	$\mathrm{O}^{(1')}\cdots\mathrm{C}^{(6')}$	352.0
$\mathrm{Cl}^{(3')}\cdots\mathrm{O}^{(1)}$	367.6	$\mathrm{O}^{(1)}\cdots\mathrm{C}^{(7')}$	348.7	$\mathrm{O}^{(1')}\cdots\mathrm{C}^{(5')}$	356.1
$\mathrm{Cl}^{(3')}\cdots\mathrm{C}^{(7)}$	373.0	$\mathrm{O}^{(1)}\cdots\mathrm{C}^{(5)}$	361.1	$\mathrm{O}^{(1')}\cdots\mathrm{C}^{(10')}$	361.3
$\mathrm{Cl}^{(3')}\cdots\mathrm{C}^{(5)}$	379.5	$\mathrm{O}^{(1)}\cdots\mathrm{C}^{(10)}$	396.7	$\mathrm{O}^{(1')}\cdots\mathrm{O}^{(1')}$	385.9
$\mathrm{Cl}^{(3')}\cdots\mathrm{C}^{(8')}$	397.3	$\mathrm{O}^{(1)}\cdots\mathrm{C}^{(4)}$	400.3	$\mathrm{O}^{(1')}\cdots\mathrm{C}^{(9')}$	398.2
$\mathrm{Cl}^{(3')}\cdots\mathrm{C}^{(7')}$	445.5	$\mathrm{O}^{(1)}\cdots\mathrm{C}^{(6')}$	402.1	$\mathrm{O}^{(4')}\cdots\mathrm{C}^{(6)}$	344.8
$\mathrm{O}^{(4)}\cdots\mathrm{O}^{(4)}$	380.8	$\mathrm{O}^{(4)}\cdots\mathrm{C}^{(3)}$	340.5	$\mathrm{O}^{(4')}\cdots\mathrm{C}^{(6')}$	348.5
$\mathrm{O}^{(4)}\cdots\mathrm{O}^{(1)}$	380.9	$\mathrm{O}^{(4)}\cdots\mathrm{C}^{(8)}$	352.3	$\mathrm{O}^{(4')}\cdots\mathrm{O}^{(1')}$	373.5
$\mathrm{O}^{(4)}\cdots\mathrm{C}^{(2)}$	399.9	$\mathrm{O}^{(4)}\cdots\mathrm{C}^{(7)}$	356.3	$\mathrm{O}^{(4')}\cdots\mathrm{C}^{(5')}$	382.3
		$\mathrm{O}^{(4)}\cdots\mathrm{C}^{(4)}$	367.8	$\mathrm{O}^{(4')}\cdots\mathrm{C}^{(7)}$	390.6

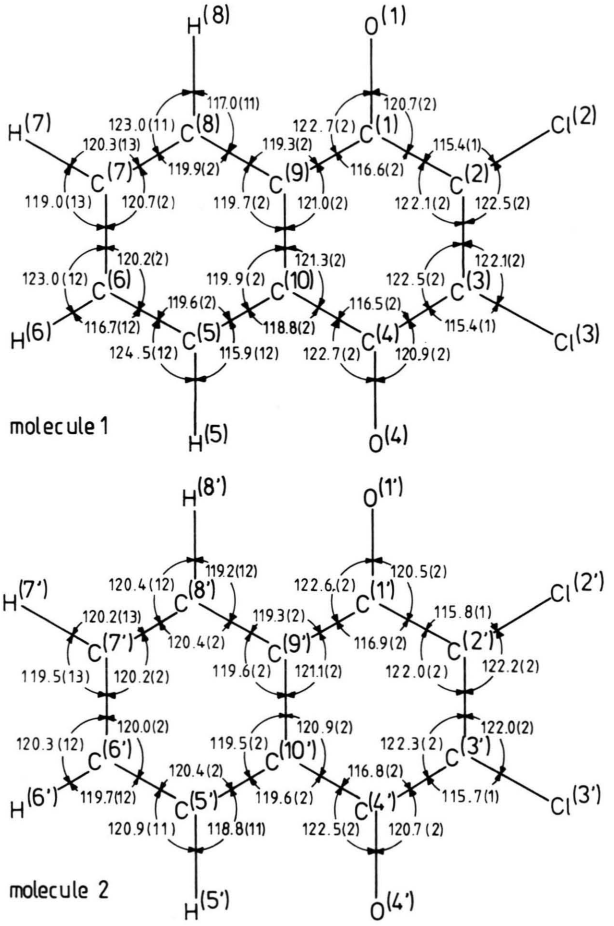

Fig. 6. Bond angles (in angular degrees) the molecules of 2,3-dichloro-1,4-naphthoquinone of phase I (molecules **1** and **2**).

and $O^{(4)}$, respectively $Cl^{(2')}$, $Cl^{(3')}$, $O^{(1')}$ and $O^{(4')}$, from the ring plane is in the range $-4.85 \leqq d/\text{pm} \leqq 10.55$.

The intramolecular geometry (bond distances and bond angles, respectively) are shown in Figs. 5 and 6. The C–Cl bond lengths are $C^{(2)}-Cl^{(2)} = 170.9(2)$ pm and $C^{(3)}-Cl^{(3)} = 170.6(2)$ pm, respectively $C^{(2')}-Cl^{(2')} = 170.6(2)$ pm and $C^{(3')}-Cl^{(3')} = 171.0(2)$ pm. No significant difference can be found between the molecular geometries in I and II reported by Ikemoto et al. [2]. The C–C bond lengths are separated in two groups. In the ring $C^{(5)} \cdots C^{(10)}$ they are in the range $137.2 \leqq d_{C-C}/\text{pm} \leqq 140.0$ for I and $135.9 \leqq d_{C-C}/\text{pm} \leqq 141.1$ for II. In contrast, the localized single bonds $C^{(1)}-C^{(2)}$, $C^{(3)}-C^{(4)}$, $C^{(4)}-C^{(10)}$, and $C^{(9)}-C^{(1)}$ have bond lengths $147.7 \leqq d_{C-C}/\text{pm} \leqq 149.9$ for I and $146.9 \leqq d_{C-C}/\text{pm} \leqq 150.0$ for II; the length of the localized double bond $C^{(2)}-C^{(3)}$ is 133.6(3) pm for both molecules of the asymmetric unit of I and 131.3(9) pm, respectively 134.1(9) pm for II. In both phases the C=O bond lengths are within $119.7 \leqq d_{C=O}/\text{pm} \leqq 121.2$; the C–Cl bond lengths are in the range $169.5 \leqq d_{C-Cl}/\text{pm} \leqq 172.7$.

There are several intermolecular contacts within the van der Waals distances obtained; they are listed in Table 6.

Phase II of 2,3-Cl_2-1,4-$O_2C_{10}H_4$, which crystallizes in the orthorhombic polar space group C_{2v}^5-$Pb2_1a$ with $Z = 8$, shows a four line ^{35}Cl NQR spectrum, too. Again, there is no discontinuity in the $\nu_i = f(T)$ curves ($i = 1, 2, 3, 4$). The results of the NQR spectroscopy are in complete agreement with the crystal structure of II [2].

The ^{35}Cl NQR spectra of the two phases (I and II), see Figs. 1 and 2 and Table 4, furthermore show that the molecular geometries in both phases are nearly the same. From our measurements on polycrystalline samples no assignment of the individual ^{35}Cl NQR frequencies to the four chlorine atoms in the two molecules of the asymmetric unit (both phases have two molecules in the asymmetric unit) is possible. 2,3-Cl_2-1,4-$O_2C_{10}H_4$ clearly reveals the influence of crystal field effects on the NQR spectrum. The two chlorine atoms within one molecule are chemically equivalent and the fact that in the asymmetric unit are two molecules is a pure solid state effect. Therefore, in first appoximation a one line ^{35}Cl NQR spectrum is expected for both phases. Comparing I and II, the crystal field induces a frequency difference of $\Delta\langle\nu\rangle = \langle\nu\rangle_{II} - \langle\nu\rangle_{I} = 47$ kHz at $T = 77$ K and $\Delta\langle\nu\rangle = 76$ kHz at 293 K. The temperature dependences of $\nu(^{35}Cl)$ are very similar in both phases: $d\nu/dT = 2.2 \cdots 2.5$ kHz/K for I and $2.0 \cdots 2.4$ kHz/K for II. The slightly stronger overall decrease of $\langle\nu\rangle$ with temperature found for I compared to II reflects the slightly more dense molecular packing in II. On the other hand, the ^{35}Cl NQR frequency spread is large, $\nu_{max} - \nu_{min} = 348$ kHz at 77 K (408 kHz at 293 K) in I and 264 kHz at 77 K (180 kHz at 293 K) in II. The overall splitting (phases I and II) is as large as 348 kHz at 77 K and 408 kHz at 293 K. This shows that, without a knowledge of the crystal structures, differences of 500 kHz in the ^{35}Cl NQR frequencies for chemically equivalent chlorine atoms bound to carbon are out of a quantitative discussion and the "loose" description of such an observation as due to crystal field effects is appropriate.

The dependence of the NQR frequencies (at 77 K) on the bond lengths C – Cl for chlorine atom bound to an sp^2 carbon atom gives quite a satisfactory correlation as found for chloro-2,5-cyclohexadiene-1,4-diones and chloro-2,5-cyclohexadiene-1-ones [8]. The ^{35}Cl NQR frequencies (at 77 K, see Table 4) of the two phases (I and II) of 2,3-Cl_2-1,4-$O_2C_{10}H_4$ and the corresponding intramolecular distances (see Fig. 5) correlate quite well according to the theory:

$$\nu(^{35}\mathrm{Cl}) \sim (d_{(\mathrm{C-Cl})})^{-3}. \qquad (3)$$

For a number of chloro-cyclohexadiene-diones and chloro-cyclohexadiene-ones, we find [8, this paper]

$$\begin{aligned}\nu\,(^{35}\mathrm{Cl})/\mathrm{MHz} \\ &= a/\mathrm{MHz} + b/(\mathrm{MHz}\cdot\mathrm{pm}^3)\cdot(d_{(\mathrm{C-Cl})}/\mathrm{pm})^{-3} \\ &= (7 \pm 10) + (153 \pm 78)\cdot 10^6\,(d_{(\mathrm{C-Cl})}/\mathrm{pm})^{-3}, \qquad (4)\end{aligned}$$

where ν is given in MHz, a in MHz, and b in MHz pm^3. The slope of the curve, b, is $(153 \pm 78)\cdot 10^6$ MHz pm^3, determined by least squares adjustment which includes 35 ^{35}Cl NQR frequencies measured on 14 different compounds. The strong deviation from (4), observed in [8] for I of 2,3-Cl_2-1,4-$O_2C_{10}H_4$, lead us to the refinement of the crystal structure. It seems, that it was worth while to do it.

Pyroelectricity of 2,3-*Dichloro*-1,4-*naphthoquinone*

According to the crystal structure of II determined by Ikemoto et al. [2] the polar 2_1-axis is the ***b***-axis of the crystal. The pyroelectric coefficient $p^x(T)$ was measured. Figure 3 reveals a slight increase of $p^x(T)$ with increasing temperature. The $p^x(T)$ curve is characteristic for an organic solid which has no phase transition in the whole range of T covered. The pyroelectric coefficient, for example, of 1-chloro-3-nitrobenzene is of the same magnitude ($p^x/\mu\mathrm{C\,m^{-2}\,K^{-1}}$: 5.7 ⋯ 10.2 ($100 \leqq T/\mathrm{K} \leqq 310$)) [3].

We are grateful to the Stiftung Volkswagenwerk and to the Founds der Chemischen Industrie for support of this work and to Dr. H. Paulus for collecting sets of X-ray diffraction intensities.

[1] J. C. Métras, Acta Cryst. **14,** 153 (1961).
[2] I. Ikemoto, K. Yakushi, Y. Naito, H. Kuroda, and M. Sano, Acta Cryst. **B 33,** 2076 (1977).
[3] Al. Weiss and S. Fleck, Ber. Bunsenges. Phys. Chem. **91,** 913 (1987).
[4] S. B. Lang, Sourcebook of Pyroelectricity, Gordon and Breach Publ., London 1974. – R. L. Byer and C. R. Roundy, Ferroelectrics **3,** 333 (1972).
[5] N. P. Hartley, P. T. Squire, and E. H. Putley, J. Phys. **E 5,** 229 (1972).
[6] P. Bray, S. Moskowitz, H. Hooper, R. Barnes, and S. Segel, J. Chem. Phys. **28,** 99 (1958).
[7] K. J. van Weperen and G. J. Visser, Acta Cryst. **B 28,** 338 (1972).
[8] S. Brummer, H. Paulus, and Al. Weiss, Z. Naturforsch. **43 a,** 873 (1988).